

## Failure of the Woods-Saxon nuclear potential to simultaneously reproduce precise fusion and elastic scattering measurements

A. Mukherjee,<sup>1,\*</sup> D. J. Hinde,<sup>1</sup> M. Dasgupta,<sup>1</sup> K. Hagino,<sup>2</sup> J. O. Newton,<sup>1</sup> and R. D. Butt<sup>1</sup>

<sup>1</sup>*Department of Nuclear Physics, Research School of Physical Sciences and Engineering,  
Australian National University, Canberra, ACT 0200, Australia*

<sup>2</sup>*Department of Physics, Tohoku University, Sendai 980-8578, Japan*

(Received 29 January 2007; published 20 April 2007)

A precise fusion excitation function has been measured for the  $^{12}\text{C}+^{208}\text{Pb}$  reaction at energies around the barrier, allowing the fusion barrier distribution to be extracted. The fusion cross sections at high energies differ significantly from existing fusion data. Coupled reaction channels calculations have been carried out with the code FRESKO. A bare potential previously claimed to uniquely describe a wide range of  $^{12}\text{C}+^{208}\text{Pb}$  near-barrier reaction channels failed to reproduce the new fusion data. The nuclear potential diffuseness of 0.95 fm which fits the fusion excitation function over a broad energy range fails to reproduce the elastic scattering. A diffuseness of 0.55 fm reproduces the fusion barrier distribution and elastic scattering data, but significantly overpredicts the fusion cross sections at high energies. This may be due to physical processes not included in the calculations. To constrain calculations, it is desirable to have precisely measured fusion cross sections, especially at energies around the barrier.

DOI: [10.1103/PhysRevC.75.044608](https://doi.org/10.1103/PhysRevC.75.044608)

PACS number(s): 25.70.Jj, 24.10.Eq

### I. INTRODUCTION

Knowledge of the internuclear potential, as a function of the separation of the colliding nuclei, is a key ingredient in the analysis of nuclear reactions. Consisting of the repulsive Coulomb and centrifugal potentials and the attractive nuclear potential, the main challenge is to determine the nuclear potential.

There are different approaches to determine the nuclear potential theoretically, for example the double folding model [1] or proximity potential [2]. To obtain experimental information on the nuclear potential, it is common to fit data with a parameterized Woods-Saxon (WS) form, which can reproduce quite well double-folding model calculations [3]. Potential parameters have been obtained from analysis of elastic scattering data [1], or more recently from precisely measured fusion excitation functions [4]. While analyzing the elastic scattering data, one normally fits the elastic angular distributions using an optical potential with its real and imaginary parts described by WS shapes. Because of the strong absorption in heavy-ion reactions, the angular distributions for elastic scattering are most sensitive to the tail region of the potential. The primary condition for fusion is that the colliding system should overcome the fusion barrier and reach the internal potential pocket. This means that in general the fusion process is sensitive to the potential at smaller internuclear separations than the elastic scattering. It has been found [1] that the best fits to the elastic scattering data are usually obtained with a diffuseness of around 0.63 fm. This value of the diffuseness parameter is consistent with (and perhaps guided by) the nuclear potentials calculated from the double folding model [1].

It is well established [5] that the fusion process, like the more peripheral processes, is strongly influenced by the internal degrees of freedom of the colliding nuclei, such as vibration, rotation, and transfer of nucleons between the interacting nuclei. The coupling of the elastic channel to these internal degrees of freedom, at energies below the average fusion barrier, leads to an enhancement of fusion cross sections ( $\sigma_{\text{fus}}$ ) relative to those expected from a single barrier penetration calculation. This can be understood within the eigenchannel approximation as resulting from the effect of channel couplings, which replaces the single one-dimensional fusion barrier by a distribution of barriers above and below the uncoupled fusion barrier.

It was shown by Rowley *et al.* [6] that a fusion barrier distribution  $D(E)$ , resulting from channel couplings, could be extracted from a precisely measured fusion excitation function.  $D(E)$  is obtained by taking the second derivative of the product of center-of-mass energy and the fusion cross section ( $E\sigma_{\text{fus}}$ ) with respect to the center-of-mass energy  $E$  (represented as  $E_{\text{c.m.}}$  in figures for clarity). Determining  $D(E)$  hence demands very precisely determined fusion cross sections. Such measurements were pioneered by Leigh *et al.* [7], and have been extensively used to understand the fusion mechanism in a wide range of reactions [5]. The centroid of the measured fusion  $D(E)$  gives the average fusion barrier ( $B_0$ ), which is therefore a well determined experimental quantity when a precisely measured fusion excitation function is available [8,9].

The enhancement in experimental precision and accuracy required to measure barrier distributions, together with sensitivity of calculations to the nuclear potential used, has led to renewed interest in the exact form of the nuclear potential in heavy-ion collisions. Systematic fitting of high precision fusion data for many reactions, at energies above the fusion barrier region, has shown that a nuclear potential having a diffuseness of at least 0.8–1.1 fm is required to fit the high

\*Permanent address: Saha Institute of Nuclear Physics, 1/AF, Bidhan Nagar, Kolkata-700064, India.

energy part of the fusion excitation functions [4,10]. The reason for needing a different potential diffuseness when fitting elastic scattering or fusion data for the same system has remained an unresolved question, since it was first noted over a decade ago.

Because of the intensive time-consuming nature of realistic calculations, only a few efforts [11–15] have been made to reproduce simultaneously elastic scattering and fusion cross sections for heavy systems using the same potential. To our knowledge, no such analyses have been carried out for reactions where high precision fusion cross sections are available. As will be discussed in this paper, the most reliable approach to obtain a single set of potential parameters for a given reaction might lie in fitting elastic scattering angular distributions for a given system, but constrained by the experimental  $B_0$  obtained from high precision fusion cross section measurements.

Recently, an extensive investigation [16] was undertaken to measure and explain a broad range of elastic, inelastic, transfer and fusion cross sections for the  $^{12}\text{C}+^{208}\text{Pb}$  reaction at energies around the barrier, using the coupled reaction channels (CRC) framework. An energy-independent bare nuclear potential of the WS form was used:

$$V_N(r) = -V_0 / (1 + \exp[(r - r_0 A_p^{1/3} - r_0 A_T^{1/3})/a]), \quad (1)$$

with  $V_0$ ,  $r_0$  and  $a$  being the depth, radius and diffuseness parameters. The potential, with parameters  $V_0 = 50$  MeV,  $r_0 = 1.2$  fm, and  $a = 0.63$  fm, was claimed to give a satisfactory reproduction of all the data, and thus to be “the unique nucleus-nucleus potential for the  $^{12}\text{C}+^{208}\text{Pb}$  system” [16]. This conclusion is very interesting, as it seems to be an exception to the broad systematics [4] which show that different  $a$  values are needed to reproduce elastic scattering and fusion. However, the number of fusion cross sections available in Ref. [16] were limited, and had relatively large error bars. Therefore, with the aim of determining a very reliable  $B_0$  and obtaining a deeper insight into the nuclear potentials determined from elastic scattering and fusion data, a precise measurement of the fusion excitation function for the  $^{12}\text{C}+^{208}\text{Pb}$  reaction was carried out.

## II. EXPERIMENTAL PROCEDURE AND RESULTS

The experiment was performed with a pulsed beam of  $^{12}\text{C}$  (1 ns wide beam bursts separated by 640 ns), from the 14UD tandem accelerator at the Australian National University.  $^{12}\text{C}$  beams, in the energy range 58–94 MeV, were incident on enriched (>99%)  $^{208}\text{PbS}$  targets, of thickness  $\sim 84 \mu\text{g}/\text{cm}^2$ , evaporated onto a  $\approx 15 \mu\text{g}/\text{cm}^2$  C backing. For normalization, two monitor detectors, placed at angles of  $22.5^\circ$  above and below the beam axis, measured the elastically scattered beam particles. The compound nucleus formed following fusion results in both fission fragments and evaporation residue (ER) formation. Thus in the experiment, fission, and ER cross sections were determined by detecting the corresponding products consecutively for the same beam energy.

Fission fragments following fusion were detected in the CUBE detector array [17], using a large area (357 mm  $\times$

284 mm) position sensitive multiwire proportional counter covering laboratory angles from  $95^\circ$ – $170^\circ$ . However, the measurements were restricted to the angular range  $95^\circ$ – $165^\circ$ , since an annular silicon surface barrier detector was placed 8 cm from the target, at a mean angle of  $174^\circ$ , to detect the decay  $\alpha$ -particles from the evaporation residues. For the ER measurements, a target backed by an Al catcher foil was used; the Al foil was  $550 \mu\text{g}/\text{cm}^2$  in thickness, so as to stop the recoiling heavy residues well within the foil. The reaction products were identified by their distinctive  $\alpha$ -energies and half-lives (182 ns to 23.9 m).

The observed ER products were  $xn$ ,  $p2n$ , and  $\alpha xn$  (associated with both fusion evaporation and incomplete fusion, if any [18]). The total ER and fission excitation functions are plotted (solid points) in Fig. 1(a), together with the results from the previous measurements (open points) [16,19]. The fusion cross sections  $\sigma_{\text{fus}}$  were determined by summing the ER and fission cross sections. The measured ratios of the fission to ER cross sections are shown in Fig. 1(b). The smooth systematic behavior of this ratio allowed determination of the ER cross section at  $E = 58.32$  MeV, where only the fission cross section

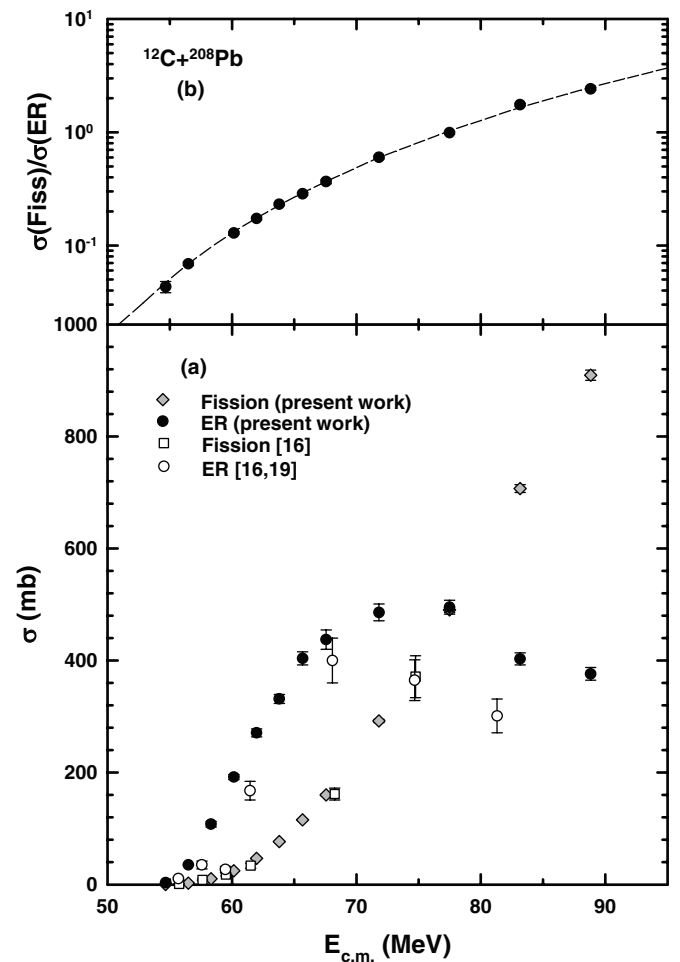


FIG. 1. (a) The evaporation residue (ER) and fission cross sections as a function of center-of-mass energy for the  $^{12}\text{C}+^{208}\text{Pb}$  reaction. (b) The ratio of the fission to ER cross sections for the present measurement. The line is drawn to guide the eye.

TABLE I. Fission, ER, and fusion cross sections for  $^{12}\text{C}+^{208}\text{Pb}$  determined in this work; quoted errors reflect statistical uncertainties only. The c.m. energies ( $E$ ) are the values after correcting for energy loss in the target. The value of  $\sigma_{\text{ER}}$  at  $E = 58.32$  MeV was obtained by interpolation (see text).

$E_{\text{beam}}$ (MeV)	$E$ (MeV)	$\sigma_{\text{fiss}}$ (mb)	$\sigma_{\text{ER}}$ (mb)	$\sigma_{\text{fus}}$ (mb)
57.87	54.67	$0.137 \pm 0.003$	$3.18 \pm 0.36$	$3.32 \pm 0.36$
59.80	56.49	$2.42 \pm 0.03$	$35.2 \pm 1.2$	$37.6 \pm 1.2$
61.73	58.32	$10.4 \pm 0.1$	$108 \pm 5$	$118 \pm 5$
63.66	60.15	$24.7 \pm 0.2$	$192 \pm 5$	$217 \pm 5$
65.59	61.97	$46.9 \pm 0.5$	$271 \pm 7$	$318 \pm 7$
67.52	63.80	$76.6 \pm 0.8$	$331 \pm 8$	$408 \pm 8$
69.50	65.67	$115 \pm 1$	$404 \pm 12$	$519 \pm 12$
71.50	67.56	$160 \pm 2$	$438 \pm 17$	$598 \pm 17$
76.00	71.82	$292 \pm 3$	$486 \pm 15$	$778 \pm 15$
82.00	77.49	$491 \pm 5$	$495 \pm 12$	$986 \pm 13$
88.00	83.16	$707 \pm 7$	$403 \pm 11$	$1110 \pm 13$
94.00	88.83	$910 \pm 9$	$376 \pm 12$	$1286 \pm 15$

was obtained. Conservatively, a 5% uncertainty was assigned to this ER cross section.

The present ER, fission, and fusion cross sections are presented in Table I with statistical uncertainties, and the  $\sigma_{\text{fus}}$  are shown in Figs. 2(a) and 2(b). The maximum systematic uncertainty for the ER cross sections is  $\pm 5\%$ , and  $\pm 2\%$  for the fission cross sections. Thus at the highest energies,  $\sigma_{\text{fus}}$  will have a total systematic uncertainty of  $\pm 3\%$ . The figures also show  $\sigma_{\text{fus}}$  from earlier works (open points) [16,20]. The center-of-mass energies  $E$  have been corrected for energy loss in the target. The fission cross sections of Santra *et al.* [16] agree with the present data, but the ER cross sections [19] used in that work are significantly lower than the present measurements. This difference in ER cross sections leads to the significant difference in the fusion cross sections seen in the figures.

The fusion  $D(E)$ ,  $d^2(E\sigma_{\text{fus}})/dE^2$  was obtained from the fusion excitation function of the present work using a point difference formula [7], and is shown in Fig. 2(c). For extracting  $D(E)$ , the energy step lengths used were in the range 1.7–1.9 MeV up to  $E = 60.15$  MeV, and 3.4–3.8 MeV above 60.15 MeV. The average barrier energy,  $B_0$  was obtained from single-barrier penetration model fits to the fusion cross sections above 200 mb. The nuclear potential required for the calculations was taken to be of Woods-Saxon form, given by Eq. (1). The potential parameters were obtained by fixing  $r_0$  to 1.07 MeV, and varying  $a$  and  $V_0$  to obtain a good fit to the high energy part of the cross sections. These are discussed in Sec. III C. This fitting procedure yielded  $B_0 = 57.0 \pm 0.4$  MeV.

### III. COUPLED REACTION CHANNELS ANALYSIS

With the aim of reproducing simultaneously the existing elastic scattering data [16] and the precisely measured fusion excitation function and fusion barrier distribution of the present work, CRC calculations were performed using a real energy independent bare Woods-Saxon potential. These

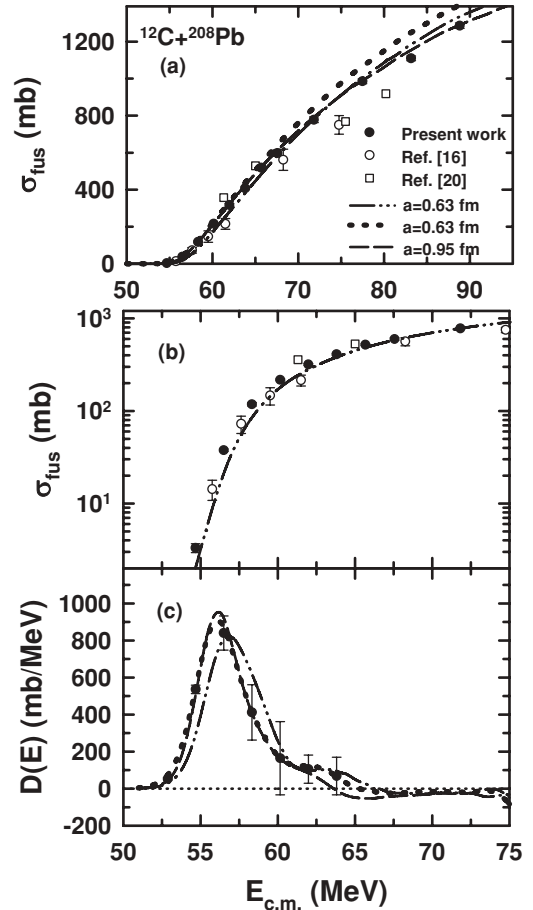


FIG. 2. Measured and calculated fusion excitation functions and barrier distributions for the  $^{12}\text{C}+^{208}\text{Pb}$  reaction. The lines show the FRESKO calculations using different potential parameter sets. See text for details.

were carried out using the code FRESKO [21]. Calculating both elastic and fusion observables within the same CRC model, a single real nuclear potential with couplings should in principle be able to reproduce both data sets. In practice, it is not possible to include all conceivable couplings in CRC calculations. In the following calculations the significant low energy vibrational and transfer couplings are included. Couplings to high energy states (e.g., giant resonances) that lead to a dynamical polarization potential (DPP) or potential renormalization are not included here—nor are they included in general in CRC calculations. However, since in this work the nuclear potential is obtained by fitting the experimental data, the DPP generated by such couplings is effectively included in this empirical bare potential. Thus in the present CRC calculations, it is reasonable to expect that such an empirical bare potential with couplings only to low-lying states should simultaneously describe the fusion and elastic scattering data.

#### A. Baseline calculation

A WS bare potential was used in Ref. [16] to describe simultaneously, in a full CRC framework, the measured fusion, elastic and other reaction channels for the  $^{12}\text{C}+^{208}\text{Pb}$

reaction. As a baseline, the same calculations were repeated in the present work. The coupling scheme, as described in Ref. [16], includes inelastic couplings to the  $3^-$ ,  $5^-$ , and  $2^+$  states of  $^{208}\text{Pb}$  and to a few states of the outgoing transfer partitions ( $^{13}\text{C}+^{207}\text{Pb}$ ,  $^{11}\text{B}+^{209}\text{Bi}$ , and  $^8\text{Be}+^{212}\text{Po}$ ). The coupling strengths, and the spectroscopic factors for all the transfer partitions, were the same as used in Ref. [16]. The optical potentials in the elastic and inelastic channels were assumed to be identical, comprising the real bare WS potential with parameters  $V_0 = 50$  MeV,  $r_0 = 1.2$  fm, and  $a = 0.63$  fm, and a WS squared imaginary potential of depth 50 MeV, radius parameter 1.0 fm and diffuseness parameter 0.4 fm [16]. The small radius parameter of the imaginary potential means that loss of flux due to the imaginary potential occurs almost exclusively inside the fusion barrier radius, ensuring that any surface interactions are essentially due to the couplings. Thus, defining fusion as the flux loss resulting from the imaginary potential should be a good approximation.

The results of this calculation are shown in Figs. 2 and 3 by the dot-dot-dashed curves. It is worth noting that the results of these calculations agree almost exactly (as would be hoped) with those presented in Ref. [16]. Figure 2(a) and 2(b) show that, averaged over beam energy, the fusion cross sections measured in this work appear to be reasonably well reproduced (much better than the previous data available in Ref. [16]). However, the calculated cross sections are systematically low at the lower energies. The significance of this discrepancy is highlighted in Fig. 2(c), where a comparison of  $D(E)$  extracted from the new fusion data with that calculated using this potential (dot-dot-dashed curve) reveals clearly that the calculation gives a fusion barrier distribution that is higher in energy than the measured  $D(E)$ . Figure 3 shows that despite this, the calculation reproduces rather well the elastic scattering angular distribution data at two bombarding energies,  $E_{\text{lab}} = 69.9$  and 84.9 MeV, as also concluded in Ref. [16]. However, the mismatch with the new fusion data indicates that the real potential is inappropriate, and thus the agreement of the calculation with the measured elastic scattering is not so meaningful.

To attempt to simultaneously reproduce the fusion and elastic scattering data by changing the real potential parameters, we now impose as the primary criterion that the calculation should match the measured average fusion barrier energy and barrier distribution.

### B. Matching $D(E)$

Upon adjusting the radius parameter of the WS potential from 1.20 to 1.218 fm, the barrier distribution can be reproduced very well, as shown by the short dashed line in Fig. 2(c). However, Fig. 2(a) shows that now the calculated high energy fusion cross sections are much larger than those measured. Furthermore, the calculated elastic scattering (Fig. 3) is now lower than the data at both energies.

This clearly demonstrates that although the calculations with the real potential diffuseness of 0.63 fm, as used by Santra *et al.*, can reproduce reasonably well the elastic, inelastic, and transfer angular distribution, they cannot accurately reproduce the fusion excitation function. Thus this real potential cannot

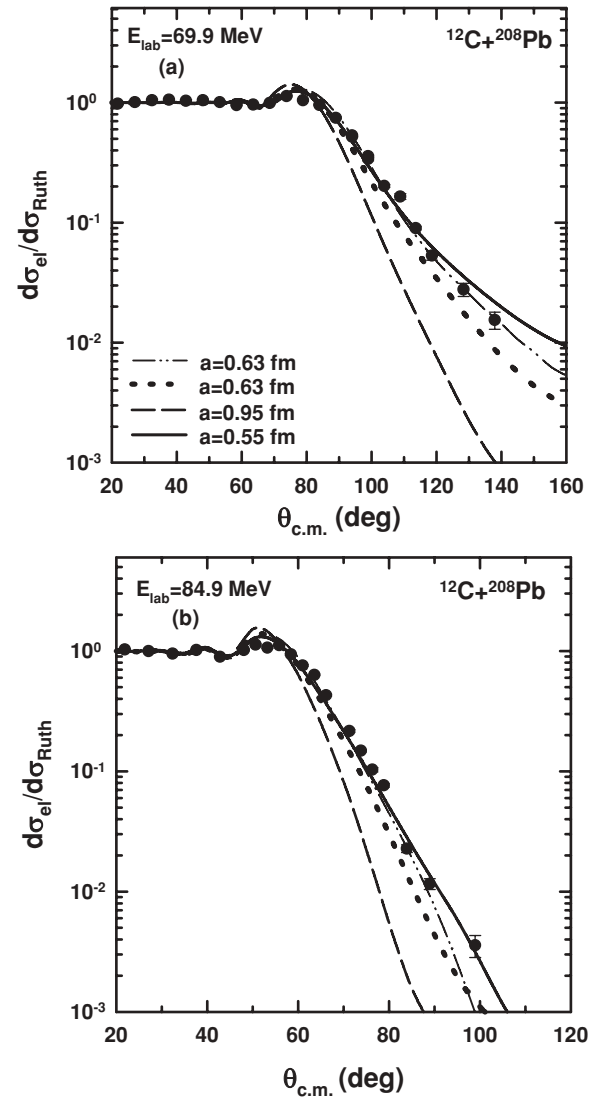


FIG. 3. The elastic scattering angular distribution at laboratory energies of (a) 69.9 MeV and (b) 84.9 MeV. The data are taken from Ref. [16]. The lines show the FRESKO calculations using different sets of potential parameters. See text for details.

be “the unique potential” that reproduces all observables for the  $^{12}\text{C}+^{208}\text{Pb}$  reaction.

The systematic overprediction of the measured precision fusion data by calculations using a WS potential diffuseness in the range 0.6 to 0.7 has recently been highlighted for many reactions [4]. Having matched the barrier energy, the comparison of fusion data with the calculation for the  $^{12}\text{C}+^{208}\text{Pb}$  reaction now agrees with this seemingly universal behavior. To reproduce the above-barrier fusion cross sections within the accepted coupled-channels framework, currently the only recourse [4] is to use a substantially larger real potential diffuseness.

### C. Matching $D(E)$ and high energy $\sigma_{\text{fus}}$

Calculations to reproduce the fusion excitation function and  $D(E)$  were first carried out without including couplings,

making the parameter searching procedure much quicker. For consistency with the previous calculations, potential depths were constrained to be below 100 MeV. A potential with  $a = 0.95$  fm,  $V_0 = 86$  MeV, and  $r_0 = 1.07$  fm reproduced well the average barrier and high energy  $\sigma_{\text{fus}}$ . On including couplings in coupled-channels calculations not using the eigenchannel approximation, the average barrier is shifted to a lower energy (equivalent to a dynamical polarization potential). With the same couplings as in the baseline calculations, both  $D(E)$  and the above-barrier  $\sigma_{\text{fus}}$  were reproduced for  $a = 0.95$  fm with a depth adjusted to 79 MeV. The excellent matching with the experimental fusion data is shown in Fig. 2(a) and 2(c) by the long dashed curves. However, Fig. 3 shows that the calculations completely fail to reproduce the measured elastic scattering angular distributions, not only at the largest angles, but also in the region before the main falloff of  $d\sigma_{el}/d\sigma_{\text{Ruth}}$ .

Interestingly, although the fusion cross sections are smaller for  $a = 0.95$  fm compared to  $a = 0.63$  fm, the elastic scattering yield at the larger angles is also smaller. This is a result of Fresnel diffraction. This “missing flux” in the elastic channel in fact appears at angles forward of the main falloff in yield, resulting in the calculated  $d\sigma_{el}/d\sigma_{\text{Ruth}}$  being substantially larger than unity (and larger than the experimental values).

The above sets of calculations show unambiguously for the  $^{12}\text{C} + ^{208}\text{Pb}$  reaction that fitting the above-barrier part of the fusion excitation function requires a large diffuseness ( $\sim 0.95$  fm) which cannot reproduce the elastic scattering data. In contrast, fitting the elastic scattering angular distributions requires a potential with a small diffuseness ( $\sim 0.63$  fm or less). Evidence for a small nuclear potential diffuseness has recently come from analysis of deep sub-barrier quasielastic scattering data for the  $^{32}\text{S} + ^{208}\text{Pb}$  and other reactions, which also appear to require a small diffuseness parameter of around  $\sim 0.6$  fm [22]. However, such a small potential diffuseness almost universally overestimates the measured  $\sigma_{\text{fus}}$  at above-barrier energies [4].

The contradictory potential parameters required by peripheral reaction processes and the more central fusion process could in principle be explained if a WS potential form were not appropriate. Another explanation could be a dynamical process occurring at the higher partial waves (corresponding to larger overlap of the matter distributions of the two nuclei) that hinders the fusion cross sections [4]. If the latter were the case, it would be more appropriate to fit the calculations to the centroid and shape of the fusion barrier distribution, and to the elastic scattering data, but refrain from trying to reproduce the high energy fusion cross sections. This approach is carried out below.

#### D. Matching $D(E)$ and elastic scattering

Simple optical model fits to the elastic scattering data alone give a real potential diffuseness of around 0.45 fm (see Table I in Ref. [16]), suggesting that in the coupled-channels approach also, a small diffuseness should give the best fit to the elastic scattering angular distributions. In the no-coupling limit an energy independent real WS potential having parameters  $a = 0.55$  fm,  $V_0 = 70$  MeV, and  $r_0 = 1.23$  fm was found to

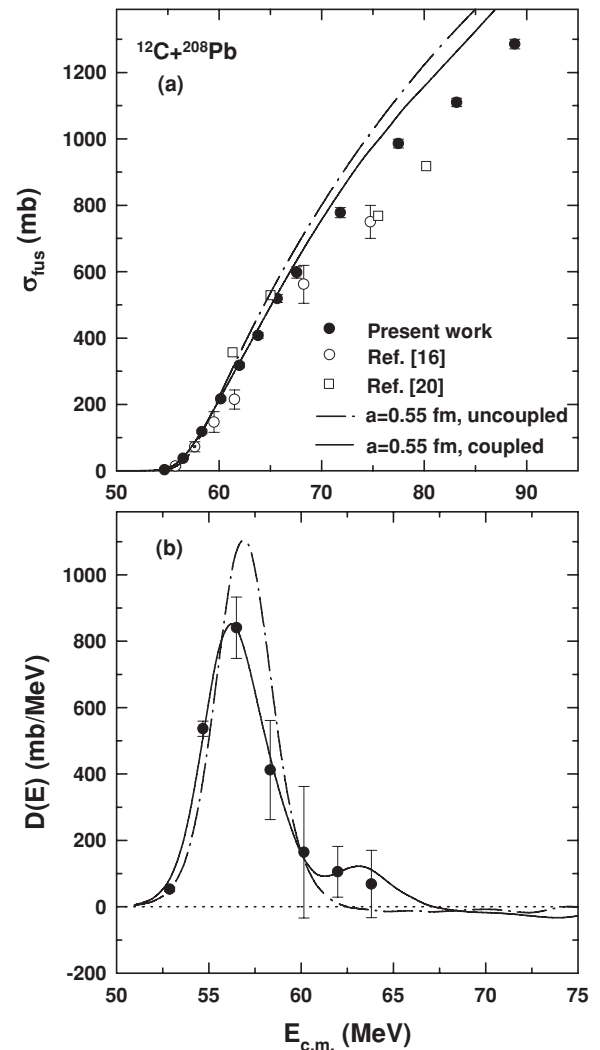


FIG. 4. As Fig. 2, for potential parameters fitting the elastic scattering data. See text for details.

reproduce the experimental average fusion barrier of 57 MeV. The results are shown by dot-dashed curves (labeled  $a = 0.55$ , uncoupled) in Fig. 4. Although the calculations with this potential, including the same couplings as before, are in reasonable agreement with the elastic scattering data, the couplings shift the average barrier lower in energy. To retain the average barrier energy, the potential depth  $V_0$  was reduced to 58 MeV. The results (labeled  $a = 0.55$ ) are shown in Figs. 3 and 4 by the full curves. Although this potential with  $a = 0.55$  fm,  $V_0 = 58$  MeV, and  $r_0 = 1.23$  fm cannot reproduce the high energy part of the fusion excitation function, it reproduces quite well the elastic scattering data, the experimental mean fusion barrier energy and the shape of the barrier distribution.

#### IV. DISCUSSION AND CONCLUSIONS

In this work, the ER, fission and fusion cross sections for the reaction  $^{12}\text{C} + ^{208}\text{Pb}$  were measured with high precision at energies around and above the barrier. Though the fission data of Ref. [16] agree well with the present measurement, there

is a significant disagreement between the two sets of ER data, which leads to a considerable difference in the fusion cross sections. Because of the high precision of the new data, a meaningful fusion barrier distribution and mean fusion barrier energy could be extracted.

Using the CRC computer code FRESKO, calculations were performed to simultaneously describe existing elastic scattering data and the new fusion excitation function and fusion barrier distribution. The real bare WS potential used in Ref. [16], which was claimed to be the unique potential that could successfully describe all near-barrier reaction channels for  $^{12}\text{C}+^{208}\text{Pb}$ , failed to reproduce the precise fusion excitation function and the average fusion barrier energy.

The elastic scattering angular distributions and the fusion barrier distribution can be reproduced by a real bare WS potential having a small diffuseness of 0.55 fm, but this overpredicts the above-barrier fusion cross sections. These can be reproduced if a large diffuseness of 0.95 fm is used, however this fails completely to reproduce the elastic scattering data. This discrepancy is consistent with a systematic analysis of separately analyzed fusion and elastic scattering data for many reactions [4].

A possible explanation of this failure of the coupled-channels model is that a WS potential form is not appropriate. Alternatively, or in addition, a dynamical process may be occurring at the highest partial waves leading to hindrance of the fusion cross sections. If the latter conjecture is correct, fitting the high energy fusion cross sections is giving an “apparent” or “effective” diffuseness of the bare real potential which is mocking up any significant physical effects not included in the coupled-channels calculations. The availability

of experimental total transfer cross sections as well as the inelastic and discrete state transfer cross sections already reported [16] for this reaction, would allow in future a complete experimental investigation of the distribution of cross sections into the different reaction channels. This may give insights into the physical processes that could be contributing to the current problem.

It is important to recognize that the analysis and conclusions in this work could only be achieved following the measurement of precise experimental fusion cross sections. In particular, data at energies near the fusion barrier allowed the mean fusion barrier energy and barrier distribution to be determined. These constrain the parameters of the real nuclear potential required by the coupled-channels model to calculate cross sections for all the reaction channels. It is therefore essential to have available precise fusion measurements when carrying out such investigations for other reactions.

#### ACKNOWLEDGMENTS

A.M. would like to thank the Saha Institute of Nuclear Physics, for providing access to the computing facilities where some of the calculations were performed. D.J.H. and M.D. acknowledge the financial support of an Australian Research Council Discovery Grant. The authors are very grateful to S. Santra for sending the detailed results of their work in tabulated form. We are grateful to Prof. N. Takigawa and Prof. J. Tostevin for useful discussions. Thanks are also due to C. R. Morton for helping with the FRESKO calculations in the beginning.

- 
- [1] G. R. Satchler and W. G. Love, *Phys. Rep.* **55**, 183 (1979); G. R. Satchler, *Nucl. Phys.* **A329**, 233 (1979).
- [2] J. Blocki, J. Randrup, W. J. Swiatecki, and C. F. Tsang, *Ann. Phys. (NY)* **105**, 427 (1977); J. Randrup and J. S. Vaagen, *Phys. Lett.* **B77**, 170 (1978).
- [3] I. I. Gontchar, D. J. Hinde, M. Dasgupta, and J. O. Newton, *Phys. Rev. C* **69**, 024610 (2004).
- [4] J. O. Newton, R. D. Butt, M. Dasgupta, D. J. Hinde, I. I. Gontchar, and C. R. Morton, *Phys. Lett.* **B586**, 219 (2004); J. O. Newton, R. D. Butt, M. Dasgupta, D. J. Hinde, I. I. Gontchar, C. R. Morton, and K. Hagino, *Phys. Rev. C* **70**, 024605 (2004), and references therein.
- [5] M. Dasgupta, D. J. Hinde, N. Rowley, and A. M. Stefanini, *Annu. Rev. Nucl. Part. Sci.* **48**, 401 (1998), and references therein.
- [6] N. Rowley, G. R. Satchler, and P. H. Stelson, *Phys. Lett.* **B254**, 25 (1991).
- [7] J. R. Leigh, M. Dasgupta, D. J. Hinde, J. C. Mein, C. R. Morton, R. C. Lemmon, J. P. Lestone, J. O. Newton, H. Timmers, J. X. Wei, and N. Rowley, *Phys. Rev. C* **52**, 3151 (1995).
- [8] M. Dasgupta, D. J. Hinde, R. D. Butt, R. M. Anjos, A. C. Berriman, N. Carlin, P. R. S. Gomes, C. R. Morton, J. O. Newton, A. Szanto de Toledo, and K. Hagino, *Phys. Rev. Lett.* **82**, 1395 (1999).
- [9] M. Dasgupta, P. R. S. Gomes, D. J. Hinde, S. B. Moraes, R. M. Anjos, A. C. Berriman, R. D. Butt, N. Carlin, J. Lubian, C. R. Morton, J. O. Newton, and A. Szanto de Toledo, *Phys. Rev. C* **70**, 024606 (2004).
- [10] C. R. Morton, A. C. Berriman, M. Dasgupta, D. J. Hinde, J. O. Newton, K. Hagino, and I. J. Thompson, *Phys. Rev. C* **60**, 044608 (1999).
- [11] S. E. Vigdor, D. G. Kovar, P. Sperr, J. Mahoney, A. Menchaca-Rocha, C. Olmer, and M. S. Zisman, *Phys. Rev. C* **20**, 2147 (1979).
- [12] M. Hugi, L. Jarczyk, B. Kamys, J. Lang, R. Müller, A. Strzalkowski, E. Ungricht, and W. Zipper, *J. Phys. G* **6**, 1257 (1980).
- [13] S. Kailas and S. K. Gupta, *Phys. Rev. C* **34**, 357 (1986).
- [14] I. J. Thompson, M. A. Nagarajan, J. S. Lilley, and M. J. Smithson, *Nucl. Phys.* **A505**, 84 (1989).
- [15] H. Esbensen, C. L. Jiang, and K. E. Rehm, *Phys. Rev. C* **57**, 2401 (1998).
- [16] S. Santra, P. Singh, S. Kailas, A. Chatterjee, A. Shrivastava, and K. Mahata, *Phys. Rev. C* **64**, 024602 (2001).
- [17] C. R. Morton, D. J. Hinde, J. R. Leigh, J. P. Lestone, M. Dasgupta, J. C. Mein, J. O. Newton, and H. Timmers, *Phys. Rev. C* **52**, 243 (1995).
- [18] A. C. Berriman, D. J. Hinde, M. Dasgupta, C. R. Morton, R. D. Butt, and J. O. Newton, *Nature (London)* **413**, 13 (2001).

- [19] T. Nomura, K. Hiruta, T. Inamura, and M. Odera, Nucl. Phys. **A217**, 253 (1973).
- [20] R. N. Sagaidak, G. N. Kniajeva, I. M. Itkis, M. G. Itkis, N. A. Kondratiev, E. M. Kozulin, I. V. Pokrovsky, A. I. Svirikhin, V. M. Voskressensky, A. V. Yerebin, L. Corradi, A. Gadea, A. Latina, A. M. Stefanini, S. Szilner, M. Trotta, A. M. Vinodkumar, S. Beghini, G. Montagnoli, F. Scarlassara, D. Ackermann, F. Hanappe, N. Rowley, and L. Stuttge, Phys. Rev. C **68**, 014603 (2003).
- [21] I. J. Thompson, Comput. Phys. Rep. **7**, 167 (1988).
- [22] K. Washiyama, K. Hagino, and M. Dasgupta, Phys. Rev. C **73**, 034607 (2006).